(*15*), further tests will be needed to determine whether this is the process used in human vision.

Second, not every relevant scene property had an influence on search. Experiments 2 and 3 showed that the direction of viewing had no effect on how easily a target could be found. We have run additional tests that generalize this result for blocks rotated 60° and 90° from those used in experiments 2 and 3.

Third, our experiments showed that visual search can be influenced by the direction of lighting in the items, although other scene properties may also be involved (*16*). As such, our results are consistent with reports (*10, 17*) that viewers are able to assign the correct direction of lighting to a scene only on the basis of intensity gradients in an image. However, our results support two stronger claims: (i) that preattentive processes determine lighting direction for objects in parallel over the image and (ii) that it is the deviation from the standard direction that is detected most readily. We also note that these effects did not require intensities to be varied smoothly (*10, 17*)—three intensities were sufficient. Perhaps the underlying processes make use of the fact that direction of lighting can be calculated by using only the orientations of the lines and the intensities of the three regions at each vertex in the image (*18*).

Taken together, these experiments imply that visual search has access to a level of representation that describes several properties of the three-dimensional scene. Therefore, search cannot be based entirely on the simple properties thought to be encoded at the earliest stages of cortical processing (for example, two-dimensional orientation, contrast, and motion registered by neurons in area 17). Either these cells are also sensitive to scene-based properties, or else visual search must access areas higher in the cortical hierarchy. In addition, these findings suggest that computational studies of vision should examine the extent to which scene properties can be computed in parallel early in the visual stream (*19*).

REFERENCES AND NOTES

1. J. Beck, in *Organization and Representation in Perception*, J. Beck, Ed. (Erlbaum, Hillsdale, NJ, 1982), pp. 285–317.
2. B. Julesz, *Trends Neurosci.* 7, 41 (1984).
3. A. Treisman, *Sci. Am.* **255**, 114B (November 1986).
4. J. T. Enns, E. P. Ochs, R. A. Rensink, *VSearch: Macintosh Software for Experiments in Visual Search* [University of British Columbia (UBC) VSearch Laboratory Vancouver, Canada, 1989].
5. Each item subtended less than 1.5°. Items were placed randomly on an imaginary 4 by 6 grid subtending 10° by 15° arc and were randomly jittered by ±0.5° to prevent influences of item collinearity.
6. Each trial began with a fixation symbol for 750 ms, followed by the display, which remained visible until the observer responded. The response was followed by accuracy feedback (a plus or minus sign), which served as the fixation point for the next trial.
7. Although each observer maintained an overall error rate of less than 10% in each condition, there were systematic differences in accuracy (Figs. 1 to 3). In particular, target-present trials led to more errors than target-absent trials, as is commonly noted [for example, R. Klein and M. Farrell, *Percept. Psychophys.* **46**, 476 (1989); G. W. Humphreys *et al.*, *J. Exp. Psychol. Gen.* **118**, 258 (1989)]. Most important for the present results, however, was the observation that errors increased with response time, indicating that observers were not simply trading accuracy for speed.
8. The response time data were analyzed as follows: First, simple regression lines were fit to the target-present and target-absent data for each observer (the average fit of these lines ranged from $r = 0.87$ to 1.00 among conditions and experiments). Second, the estimated slope and intercept parameters were submitted to analyses of variance. Finally, Fisher's least significant difference (LSD) tests were used to determine the reliability of simple effects in the context of significant main effects and interactions. The reported P values, therefore, refer to LSD tests and (by implication) to the higher order effects of which they are a part.
9. L. Kaufman, *Sight and Mind* (Oxford, New York, 1974).
10. V. S. Ramachandran, *Sci. Am.* **259**, 76 (August 1988).
11. A. Treisman and S. Gormican, *Psychol. Rev.* **95**, 15 (1988).
12. K. Nakayama and G. H. Silverman, *Nature* **320**, 264 (1986).
13. P. McLeod, J. Driver, J. Crisp, *ibid.* **332**, 154 (1988).
14. This finding is similar to the observation that briefly presented lines are detected more readily when the surrounding lines can be interpreted as a three-dimensional object [N. Weisstein and C. S. Harris, *Science* **186**, 752 (1974); J. T. Enns and W. Prinzmetal, *Percept. Psychophys.* **35**, 22 (1984)].
15. A. K. Mackworth, *Artif. Intell.* **4**, 121 (1973); *Perception* **5**, 349 (1976).
16. Strictly speaking, experiment 3 shows that search is influenced by the pattern of intensities assigned to the faces of the same three-dimensional block. Since these intensities are a joint function of the direction of lighting, surface orientation, and surface reflectance, at least one of these factors must be represented preattentively. We discuss the direction of lighting account in the text, but the other two factors may also be relevant. Consider first an account based on surface orientation. If we assume a constant direction of lighting, items can be interpreted as blocks with black, gray, and white faces. If we further assume that a three-dimensional orientation is assigned to the same-color face in each block (for example, the black face), then the face with the incongruent orientation should stand out. Alternatively, search may be governed by surface reflectance. If observers are able to group the blocks preattentively on the basis of the orientation of one of the faces, then the face with the incongruent color should stand out. We have emphasized the direction of lighting because the other two require arbitrary associations to be made between the orientations and colors of the faces of the blocks. We have neither empirical nor computational grounds to show that such associations are the basis for search.
17. J. T. Todd and E. Mingolla, *J. Exp. Psychol. Hum. Percept. Perform.* **9**, 583 (1983).
18. B. K. P. Horn, *Artif. Intell.* **8**, 201 (1977).
19. Most parallel algorithms in computational vision are based entirely on local quantities [W. E. L. Grimson, *Comput. Vis. Graph. Image Process.* **24**, 28 (1983); R. J. Woodham, *Artif. Intell.* **17**, 117 (1981)]. However, our results [experiments 1 (Fig. 1D) and 2 (Fig. 2C)] show that rapid search cannot be based only on local configurations—a consistent interpretation of the whole item is required. To determine such consistency, algorithms must use information outside the immediate neighborhood of any single location.

20. Supported by Natural Sciences and Engineering Research Council (J.E. and R.R. through R. J. Woodham) and UBC Center for Integrated Computer Systems Research (R.R.). We thank E. Ochs for programming assistance, A. MacQuistan for collecting data, and A. K. Mackworth and E. Bandari for helpful comments on earlier drafts.

12 July 1989; accepted 17 November 1989

Growth Factors Induce Phosphorylation of the Na^+/H^+ Antiporter, a Glycoprotein of 110 kD

C. SARDET, L. COUNILLON, A. FRANCHI, J. POUYSSÉGUR

The Na^+/H^+ antiporter, which regulates intracellular *p*H in virtually all cells, is one of the best examples of a mitogen- and oncogene-activated membrane target whose activity rapidly changes on stimulation. The activating mechanism is unknown. A Na^+/H^+ antiporter complementary DNA fragment was expressed in *Escherichia coli* as a β-galactosidase fusion protein, and a specific antibody to the fusion protein was prepared. Use of this antibody revealed that the Na^+/H^+ antiporter is a 110-kilodalton glycoprotein that is phosphorylated in growing cells. Mitogenic activation of resting hamster fibroblasts and A431 human epidermoid cells with epidermal growth factor, thrombin, phorbol esters, or serum, stimulated phosphorylation of the Na^+/H^+ antiporter with a time course similar to that of the rise in intracellular *p*H.

THE Na^+/H^+ ANTIPORTER IS A widespread plasma membrane transporter that regulates intracellular *p*H (pH_i) (*1, 2*) and is important in signal transduction. Its biochemical ground state is modified by oncogenic transformation and in response to a wide variety of external signals (including sperm, phorbol esters, lectins, growth factors, hormones, neurotransmitters, and chemotactic peptides) (*3–5*), resulting in a persistent cytoplasmic alkalinization (*6*). This induced *p*H change, which is most evident in the absence of bicarbonate (*7, 8*), results from an increased

Centre de Biochimie-CNRS, Parc Valrose, 06034 Nice, France.

affinity of the antiporter for H^+ at the internal H^+-regulatory site (*2, 9, 10*). To determine whether activation of the antiporter is mediated by a phosphorylation-induced conformational change (*3, 11*), we developed a specific probe for the antiporter.

The nucleotide sequence of the largest open reading frame of the human Na^+/H^+ antiporter cDNA predicts a protein of 815 amino acids with ten putative transmembrane segments followed by a long hydrophilic COOH-terminal sequence (*11–13*). To confirm this topological model, we constructed a fusion protein (Fig. 1A) of *Escherichia coli* β-galactosidase and the last 157 amino acids of the hydrophilic domain (*12, 13*). Antibodies raised against this fusion protein detected a single band of 105 to 110 kD only in cells expressing Na^+/H^+-exchange activity (Fig. 1, B and C). The PS200 clone of Chinese hamster lung (CHL) fibroblasts, which has no endogenous Na^+/H^+ antiporter activity (*14*), has been stably transfected with the human Na^+/H^+ antiporter cDNA under the control of the mouse mammary tumor virus long terminal repeat (MMTV LTR)–inducible promoter (*12*). After induction with 10 n*M* dexamethasone, we detected in the transfectant PS201 de novo expression of a 105- to 110-kD protein (Fig. 1B, lanes 1 and 2) that paralleled a 15-fold induction in Na^+/H^+ antiport activity (*15*). The clone PS127A, in which expression of the antiport protein was more prominent (Fig. 1B), overexpresses the transfected human Na^+/H^+ antiporter cDNA (*15*). This clone is derived from PS120, another CHL Na^+/H^+ antiport–deficient mutant (*14*). By immunoblotting, we also detected a protein of identical mobility in nontransfected CHL fibroblast–derived clones; the responses varied from undetectable for PS120, to weak for CCL39 parent cells, and to strong for DD12, which has a high Na^+/H^+ antiport activity (*15*). The antiporter was found to be glycosylated (Fig. 1C); treatment with neuraminidase and endoglycosidase F reduced the apparent size of the protein from 110 to 90 kD, whereas endoglycosidase H had no effect. These results are consistent with the existence of two potential N-linked glycosylation sites in the amino acid sequence (*12*) and confirm the recent observation that endoglycosidase F treatment of renal brush-border membranes specifically reduced the rate of Na^+/H^+ exchange (*16*). The higher apparent molecular mass (120 kD) for the corresponding protein detected in the human epidermoid cell line A431 (Fig. 1B) could reflect differences in glycosylation between CHL and A431 cells.

The human antiport protein expressed in stably transfected CHL fibroblasts was localized to the plasma membrane (Fig. 2). The pattern of cell fluorescence was diffuse with increased intensity at the cell periphery and lamellipodia. Permeabilization of the cells was required to detect immunoreactivity. This result is in accordance with our model, placing the long hydrophilic stretch containing the antigenic epitope inside the cell (*12*).

Fig. 2. Immunolocalization of the human Na^+/H^+ antiporter functionally expressed in CHL fibroblasts. PS120 cells transfected with the vector control (**A**) and PS127A cells that express the transfected human antiporter gene (**B**) were fixed with 3% paraformaldehyde and permeabilized with 0.2% Triton X-100. The cells were then incubated with affinity-purified RP1-c28 antibodies (1 μg/ml) and fluorescein-conjugated antibodies to rabbit immunoglobulin G (Biosys, Compiègne, France; dilution 1/200).

The Na^+/H^+ antiporter is a phosphoprotein. When CHL fibroblast and A431 cell lines were grown in the presence of [^{32}P]orthophosphate, lysed, and then subjected to immunoprecipitation and SDS–polyacrylamide gel electrophoresis (SDS-PAGE), a single phosphoprotein was apparent (Fig. 3). This phosphoprotein is the Na^+/H^+ antiporter because it had the same mobility as that revealed by immunoblotting (105 to 110 kD for CHL and 120 kD for A431 cells), and the intensity of the immunoprecipitated material paralleled expression of the Na^+/H^+ antiporter in the various CHL fibroblast–derived cell lines: no signal was detected in PS120 cells, which lack Na^+/H^+ antiport activity; a weak signal was present in the parent CCL39 cells; and a stronger signal was detected in the overexpressor DD12 cell line. The lines PS127A and DD12 have equivalent Na^+/H^+ antiport activity (10 to 15 times as large as that of the parent), yet a drastic difference in the amount of phosphoprotein present was detected (Fig. 3, lanes 3 and 4). We believe this result reflects a difference in immunoreactivity between species as, in contrast to DD12, the CHL-derived clone PS127A expresses the human antiport protein. By labeling exponentionally growing PS127A cells to equilibrium with [^{32}P]orthophosphate and [^{35}S]methionine of known specific activity, we estimated the stoichiometry of phosphorylation of the Na^+/H^+ antiporter

Fig. 1. Immunological detection of the Na^+/H^+ antiporter. (**A**) Topological model of the Na^+/H^+ antiporter showing the segment chosen to construct the antigenic fusion protein (*25*). (**B**) Immunoblotting analysis of membrane proteins from the CHL-derived clones PS201 (lanes 1 and 2) and PS127A (lane 3) and from A431 cells (lane 4). PS201 cells were grown in absence (lane 1) or presence of 10 n*M* dexamethasone for 24 hours (lane 2). Arrowhead represents the phosphorylase b standard molecular size in kilodaltons. (**C**) Immunoblotting of PS127A membrane proteins after various glycosidase treatments: lane 1 (no treatment), lane 2 (neuraminidase treatment), and lane 3 (neuraminidase and endoglycosidase F treatments). Membrane proteins (100 μg) were incubated for 4 hours at 8°C with 0.02 units of neuraminidase or with 0.25 units of endo-β-*N*-acetylglucosaminidase F or with both enzymes (Boehringer Mannheim). Arrowheads represent the molecular size of the three forms. For immunoblotting, crude membrane proteins were separated on SDS-polyacrylamide gels, electrotransferred to nitrocellulose filters, and immunoblotted as described (*26*) with a 5×10^{-3} dilution of the RP1-c28 antiserum and ^{125}I-labeled protein A. Membrane proteins (50 μg) were applied to each lane and separated by electrophoresis on 7.5% SDS-polyacrylamide gel under reduced conditions. With the exception of the human epidermoid cell line A431, the cells used in this study are all derived from CCL39 CHL fibroblasts (ATCC). The properties of the CHL-derived clones are described in the text.

to be ~1 mol of phosphate per mole of antiporter.

We next analyzed the capacity of growth factors to modify the phosphorylation state of the exchange protein. Two distinct transmembrane signal mechanisms operate in many cells including secondary cultures of CHL fibroblasts (*17*). For instance, epidermal growth factor (EGF) and thrombin use two main separate signaling pathways (*17, 18*). Because the CHL fibroblast cell line CCL39 gives only a weak response to EGF, we constructed ER22, a CCL39-derived clone that expresses a large number of human EGF receptors. In this new line of CHL fibroblasts, EGF can cause inositol lipid breakdown; however, its capacity to activate phospholipase C remains, at least, 98% lower than that of thrombin (*19*); in contrast, EGF and thrombin are equally potent for inducing mitogenesis. After a lag of 2 min, both EGF and thrombin induced a rise in pH_i that peaked at around 10 min, declined slightly thereafter, and persisted as long as the stimulus was maintained (Fig. 4A) (*6*). The in vivo state of phosphorylation of the Na^+/H^+ antiporter was analyzed under the same conditions of mitogenic stimulation by immunoprecipitation. After a lag of at least 2 min, EGF and thrombin stimulated the phosphorylation of the Na^+/H^+ antiporter in G_0-arrested ER22 cells. Both EGF- and thrombin-stimulated phosphorylation occurred on serine residues (*20*). Because this growth factor stimulation was also observed when cells were labeled to equilibrium with ^{32}P (40 hours), the increased ^{32}P incorporation into the antiporter must reflect phosphorylation of new sites on the transporter. Fetal bovine serum and phorbol esters that activate the antiporter also stimulated its phosphorylation (Fig. 4B). Identical results were obtained in quiescent CCL39 cells stimulated with serum or in A431 cells stimulated with EGF (*21*).

Thus growth factors such as EGF that activate receptor tyrosine kinases or growth factors such as thrombin that activate G protein–coupled receptors increase the phosphorylation of the Na^+/H^+ antiporter at serine residues. This finding, similar to the phosphorylation of ribosomal protein S6 (*22*), raises the possibility that there is an integrator of the diverse output signals coordinating mitogenic events. Mitogen-activated protein kinase (*23*) or Raf kinase (*24*) are potential candidates for this integrated and coordinated response. Our finding that the mitogen-induced cytoplasmic alkalinization and phosphorylation of the antiporter are temporally associated suggests that the set point value of the antiporter is rectified by phosphorylation.

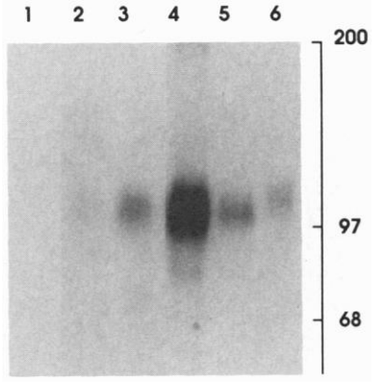

Fig. 3. Immunoprecipitation of the Na^+/H^+ antiporter from cells labeled with [^{32}P]orthophosphate. Autoradiogram of immunoprecipitates separated by electrophoresis on an SDS–7.5% polyacrylamide gel under reducing conditions. The protein content of a confluent cell layer from a 100-mm dish was applied to each lane. The cell clones used were PS120 (lane 1), CCL39 (lane 2), DD12 (lane 3), PS127 A (lanes 4 and 5), and A431 (lane 6). Lane 4 is the same as lane 5 except that the cells were labeled with ^{32}P for 1 and 20 hours, respectively. Cells grown to confluence in 100-mm dishes were labeled overnight in culture medium containing 10% fetal bovine serum (FBS) and 100 μM [^{32}P]orthophosphate (100 μCi/ml). Cells were then washed with ice-cold phosphate-buffered saline (PBS), and membrane proteins were extracted as described (*27*).

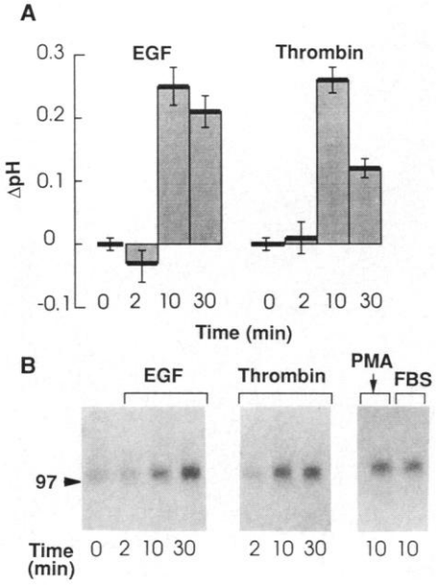

Fig. 4. Intracellular pH (**A**) and in vivo phosphorylation (**B**) of the Na^+/H^+ antiporter in mitogen-stimulated quiescent fibroblasts. These experiments were conducted on ER22, a CCL39-derived clone that expresses 800,000 human EGF receptors (*19*). ER22 cells were rendered quiescent by a 17-hour incubation in serum-free medium and were then stimulated with 40 nM EGF, 10 nM thrombin, phorbol ester (PMA) (100 ng/ml), or 10% FBS. Intracellular pH and in vivo phosphorylation were measured on parallel cultures and under the same conditions of stimulation. (A) For pH determinations, quiescent cells grown on 12 multiwell plates were incubated for 30 min in bicarbonate-free culture medium buffered with 20 mM Hepes (pH 7.4). The medium was replaced with medium containing [^{14}C]benzoic acid at time 0, and mitogen-induced pH changes were calculated as described (*28*). Error bars (±SEM) are based on triplicate determinations. (B) For immunoprecipitation, quiescent ER22 cells were labeled for 5 hours in bicarbonate- and phosphate-free culture medium containing 100 μM [^{32}P]orthophosphate (100 μCi/ml) and buffered with 20 mM Hepes (pH 7.4). After mitogenic stimulation, reactions were stopped by washing the cells three times with ice-cold PBS, and freezing the petri dishes on liquid N_2. Proteins were then extracted, solubilized, and immunoprecipitated as described (*27*). Two independent experiments have shown identical patterns of stimulated phosphorylation.

REFERENCES AND NOTES

1. P. Aronson and W. Boron, *Na^+/H^+ Exchange, Intracellular pH and Cell Function* (Academic Press, New York, 1986).
2. S. Grinstein, *Na^+/H^+ Exchange* (CRC Press, Boca Raton, FL, 1988).
3. J. Pouysségur, *Trends Biochem. Sci.* **10**, 453 (1985).
4. W. H. Moolenaar, *Annu. Rev. Physiol.* **48**, 363 (1986).
5. E. Rozengurt, *Science* **234**, 161 (1986).
6. E. Van Obberghen-Schilling, J. C. Chambard, S. Paris, G. L'Allemain, J. Pouysségur, *EMBO J.* **4**, 2927 (1985).
7. G. L'Allemain, S. Paris, J. Pouysségur, *J. Biol. Chem.* **260**, 4877 (1985).
8. M. Ganz, G. Boyarsky, R. B. Sterzel, W. Boron, *Nature* **337**, 648 (1989).
9. W. Moolenaar, R. Tsien, P. Van der Saag, S. de Laat, *ibid.* **304**, 645 (1983).
10. S. Paris and J. Pouysségur, *J. Biol. Chem.* **259**, 10989 (1984).
11. J. Pouysségur *et al.*, *Kidney Int.* **32**, S144 (1987); C. Sardet, A. Franchi, J. Pouysségur *et al.*, *Cold Spring Harbor Symp. Quant. Biol.* **53**, 1011 (1988).
12. C. Sardet, A. Franchi, J. Pouysségur, *Cell* **56**, 271 (1989).
13. A correction has to be made in the published sequence of the human Na^+/H^+ antiporter: a G at position 2442 was not previously seen. The correct sequence should read from nucleotide 2437:AAG (Lys) GGG (Gly) CAG (Gln) TAA (new stop codon). The protein codes for 815 residues instead of 894 as we reported (*12*). This error came to our attention after a full sequence of the rabbit ileal Na^+/H^+ antiporter was available [C.-M. Tse *et al.*, in preparation].
14. J. Pouysségur, C. Sardet, A. Franchi, G. L'Allemain, S. Paris, *Proc. Natl. Acad. Sci. U.S.A.* **81**, 4833 (1984).
15. A. Franchi, E. J. Cragoe, J. Pouysségur, *J. Biol. Chem.* **261**, 14614 (1986); A. Franchi, C. Sardet, J. Pouysségur, in preparation.
16. A. Yusufi, M. Szczepanska-Konkel, T. Dousa, *J. Biol. Chem.* **263**, 13683 (1988).
17. J. C. Chambard, S. Paris, G. L'Allemain, J. Pouysségur, *Nature* **326**, 800 (1987).
18. G. L'Allemain and J. Pouysségur, *FEBS Lett.* **197**, 344 (1986).
19. G. L'Allemain, K. Seuwen, T. Velu, J. Pouysségur, *Growth Factors* **1**, 311 (1989).
20. Phosphoamino acid analysis was performed under the same conditions as described in legend to Fig. 4, with three 100-mm dishes for each condition: control, 30-min stimulation with EGF, and 30-min stimulation with thrombin. The bands immunoprecipitated at 105 to 110 kD were excised from the gel, eluted, and hydrolyzed with 6N HCl. The phosphoamino acids were then separated by two-dimensional thin-layer electrophoresis as described [J. Cooper, T. Hunter, B. Sefton, *Methods Enzymol.* **99**, 387 (1983).

21. C. Sardet and J. Pouysségur, unpublished data.
22. S. Kozma *et al.*, *Cell. Signal.* **1**, 219 (1989).
23. A. Rossomando, M. Payne, M. Weber, T. Sturgill, *Proc. Natl. Acad. Sci. U.S.A.* **86**, 6940 (1989).
24. D. Morrisson *et al.*, *ibid.* **85**, 8855 (1988).
25. The fusion protein was obtained by inserting the Pvu II fragment [nucleotides 2435 to 2980 from the cDNA c28, which codes for the human Na^+/H^+ antiporter (*12*)] into the Sma I site of the PEX 3 vector (EMBL, Genofit). Large-scale production of the corresponding β-galactosidase–antiporter fusion protein was performed as described [M. Zabeau and K. Stanley, *EMBO J.* **1**, 1217 (1982). Proteins were purified by electroelution after two successive separations on SDS-PAGE. Rabbits were immunized with 100 μg of the purified protein in the presence of Freund's adjuvant by multiple subcutaneous injections on the back. The antibodies RP1-c28 were affinity-purified by incubating the antiserum with a nitrocellulose sheet coated with the fusion protein. Reacting antibodies were then eluted with glycine at 0.1*M* (*p*H 2.2) and stored at −20°C in a 50% glycerol solution in phosphate-buffered saline (PBS).
26. B. Thorens, H. Sarkar, R. Kaback, H. Lodish, *Cell* **55**, 281 (1988).
27. The frozen cell monolayer was scraped and resuspended in 500 μl of ice-cold buffer A [50 m*M* Hepes-NaOH (*p*H 7.4), 150 m*M* NaCl, 3 m*M* KCl, 12.5 m*M* sodium pyrophosphate, 10 m*M* adenosine triphosphate, 5 m*M* EDTA, 1 m*M* phenylmethylsufonyl fluoride, 1 m*M* *o*-phenanthroline, 1 m*M* iodoacetamide, and 1 μ*M* pepstatin A] and centrifuged for 15 min at 100,000*g*. The pellets were resuspended in 500 μl of ice-cold buffer A containing 1% Nikkol (Nikko Chemicals, Japan), sonicated for 40 s, and centrifuged for 30 min at 100,000*g*. The supernatants were adsorbed with protein A–Sepharose beads and then incubated for 2 hours at 4°C with 2 μg of affinity-purified RP1-c28 antibodies. A 50% suspension of protein A–Sepharose beads (50 μl) (previously incubated with a Nikkol extract of PS120 antiporter-deficient cells) was added, and the mixture was incubated for 1 hour at 4°C in a rotating shaker. The beads were then washed five times with buffer A containing 1% Nikkol, and protein was solubilized by boiling in Laemmli sample buffer.
28. G. L'Allemain, S. Paris, J. Pouysségur, *J. Biol. Chem.* **259**, 5809 (1984).
29. We thank C. Huet and D. Louvard for help with cell immunofluorescence techniques, R. Ballotti and E. Van Obberghen for technical advice on phosphoamino acid analysis, B. Contreres and B. Rossi for immunization, and M. Valetti for manuscript preparation. Supported by grants from the Centre National de la Recherche Scientifique (UPR 7300), the Institut National de la Santé et de la Recherche Médicale, the Fondation pour la Recherche Médicale, and the Association pour la Recherche contre le Cancer.

19 September 1989; accepted 4 December 1989

"... Where the speed of the elevator (S_E) is inversely proportional to the number of times the button is pushed (P_B) times the frustration constant ($_FK$).